

Assessment of advanced energy functionals in an exactly solvable model system

P. García-González

Departamento de Física Fundamental, Universidad Nacional de Educación a Distancia, Apartado de Correos 60141, E-28080 Madrid, Spain,

and European Theoretical Spectroscopy Facility

(Received 19 February 2009; published 2 June 2009)

There is an increasing interest in the use of the random-phase approximation (RPA) and extensions thereof to calculate ground-state correlation energies within the Kohn-Sham formalism. However, current implementations of these RPA-based functionals resort to the use of mean-field-like approximations when obtaining Kohn-Sham eigenorbitals and eigenenergies. In this paper we exactly calculate RPA and related results for a model system in which different correlation regimes can be easily addressed. We explore the reliability of such methods in the limit of strong interactions and pay special attention to the importance of a self-consistent resolution of the corresponding Kohn-Sham equations. In particular, we show that the self-consistent implementation of these methods provides accurate correlation energies and ground-state densities even when mean-field approximations dramatically fail.

DOI: [10.1103/PhysRevA.79.062502](https://doi.org/10.1103/PhysRevA.79.062502)

PACS number(s): 31.10.+z, 31.15.ac, 31.15.ec

I. INTRODUCTION

The Kohn-Sham (KS) formulation [1] of density-functional theory (DFT) [2] is presently a method of choice for calculating structural properties in both quantum chemistry and condensed-matter physics [3]. The KS scheme is built on the existing link between any N electron system and a noninteracting counterpart, the fictitious KS system. This link is made through the functional derivative of the so-called exchange-correlation (XC) energy functional $E_{XC}[n]$ which includes all nontrivial many-body effects of the real electron system. Since KS-DFT is an exact theory, full predictive power might be obtained as long as suitable approximations to the XC energy functional were made.

It has been argued that the heaven of chemical accuracy could be reached by using sophisticated XC functionals depending not only on the one-electron density $n(\mathbf{r})$ but also on the orbitals $\phi_n(\mathbf{r})$ and eigenenergies ε_n of the fictitious KS system [4,5]. A price to pay is the risk of missing one of the most appealing aspects of DFT, the efficiency of the popular local-density approximation (LDA) [1,6] and generalized gradient approximation (GGA) [7]. Bearing this in mind, the orbital-dependent meta-GGA functionals proposed in the last years by Perdew, Scuseria, and co-workers [8–10] offer a striking balance between computational cost and reliability. In any case, even if the spirit behind the construction of those meta-GGAs were abandoned, the use of *advanced* orbital-dependent XC functionals can be still competitive if compared, for instance, with quantum Monte Carlo, configuration interaction, or coupled cluster methods.

In general, these advanced XC functionals contain the exact exchange energy functional $E_X[n]$:

$$E_X[n] = -2 \times \frac{1}{2} \sum_{nm}^{\text{occ}} \int d\mathbf{r} d\mathbf{r}' c_{nm}(\mathbf{r}) w(\mathbf{r}, \mathbf{r}') c_{mn}(\mathbf{r}'), \quad (1)$$

where $c_{nm}(\mathbf{r}) = \phi_n^*(\mathbf{r}) \phi_m(\mathbf{r})$, $w(\mathbf{r}, \mathbf{r}')$ is the electron-electron interaction, and the factor 2 appears as a result of the sum over spin degrees of freedom (we will restrict ourselves to spin-unpolarized systems and use Hartree atomic units unless

otherwise specified). The evaluation of the functional derivative $v_X[n](\mathbf{r}) = \delta E_X[n] / \delta n(\mathbf{r})$ can be done via the optimized potential method [11], and then, the correlation energy $E_C[n] = E_{XC}[n] - E_X[n]$ is the only ingredient that must be approximated. This has to be done taking into account that the well-known compensation of errors between exchange and correlation that appears in the LDA and, to a lesser extent, in GGAs does not hold anymore. Hence, any correlation energy functional amenable to be used together with the exact exchange one [Eq. (1)] must be accurate enough by itself to provide meaningful results.

From this perspective, an interesting route is the construction of a perturbative expression of the correlation energy in terms of the KS orbitals and eigenenergies [5,12–15] much akin to the standard Møller-Plesset expansion. Other approaches can be formulated from Green's-function many-body perturbation theory [16–20] or using the so-called adiabatic connection fluctuation-dissipation theorem (ACFDT) [21–23]. The latter exactly relates the ground-state DFT correlation energy of any electron system with its density-response function. Namely,

$$E_C[n] = -\text{Im} \int_0^\infty \frac{d\omega}{2\pi} \int_0^1 d\gamma \int d\mathbf{r} d\mathbf{r}' w(\mathbf{r}, \mathbf{r}') \times [\chi_\gamma(\mathbf{r}, \mathbf{r}'; \omega) - \chi_0(\mathbf{r}, \mathbf{r}'; \omega)], \quad (2)$$

where $\chi_\gamma(\mathbf{r}, \mathbf{r}'; \omega)$ is the response of a fictitious system of electrons with the scaled interaction $\gamma w(\mathbf{r}, \mathbf{r}')$ and whose ground-state density equals the actual one. Then, $\chi_0(\mathbf{r}, \mathbf{r}'; \omega)$ is the density response of the fictitious noninteracting KS system:

$$\chi_0(\mathbf{r}, \mathbf{r}'; \omega) = 2 \sum_{nm} \frac{(f_n - f_m) c_{nm}(\mathbf{r}) c_{mn}(\mathbf{r}')}{\omega + (\varepsilon_n - \varepsilon_m) + i0^+}, \quad (3)$$

where f_n (0 or 1) are the Fermi occupation numbers. The interacting response χ_γ can be evaluated in the framework of time-dependent density-functional theory (TDDFT) [24,25]

by solving the Dyson-type equation (usual matrix operations are implied)

$$\hat{\chi}_0(\omega) = \{\hat{1} - \hat{\chi}_0(\omega)[\gamma\hat{v} + \hat{f}_{\text{XC},\gamma}(\omega)]\}^{-1}\hat{\chi}_\gamma(\omega), \quad (4)$$

where $f_{\text{XC},\gamma}(\mathbf{r}_1, \mathbf{r}_2; \omega)$ is the dynamical XC kernel of the fictitious system with the scaled interaction $\gamma\hat{v}$. Thus, any approximation to $\hat{f}_{\text{XC},\gamma}(\omega)$ defines, by construction, an ACFDT correlation energy functional. For self-consistent implementations within the KS scheme, the corresponding correlation potential $v_{\text{C}}[n](\mathbf{r}) = \delta E_{\text{C}}[n]/\delta n(\mathbf{r})$ should be evaluated accordingly [26–28].

Despite its evident computational cost, the ACFDT functionals have some appealing features. First, they are based on a formally exact expression which already contains many of the ingredients needed to describe properly electron many-body effects. Second, ground- and excited-state properties are treated under the same framework. With these motivations in mind and thanks to the growth of available computational power, the ACFDT has been applied, so far, to many different systems with very promising results. Such calculations include jellium systems [29–34], model quantum dots [35], atoms and molecules [17,19,36–44], and solids [34,45–48]. Furthermore stable and/or efficient numerical implementations of the ACFDT have been already developed [34,44,47–49]. However, almost all of these calculations have been performed in a non-self-consistent post-LDA or -GGA fashion because the evaluation of the ACFDT correlation potential is a formidable task. Actually, ACFDT correlation potentials have been only evaluated for model electron systems [35,50], atoms [37], and simple bulk crystalline solids [51], either neglecting $\hat{f}_{\text{XC},\gamma}(\omega)$ [which is formally equivalent to the random-phase approximation (RPA), that is, to the resummation of the so-called ring diagrams in the language of many-body theory] or using very simple approximations to the XC kernel. Moreover, a detailed assessment of the self-consistent implementation of ACFDT when LDA or GGA orbitals are not accurate at all has not been performed yet. Another problem is that, as it is already known, some model XC kernels which provide reasonable excited-state spectra are not suitable for correlation energy calculations and vice versa. Finally, the success of the ACFDT when studying dissociation processes (dispersion van der Waals forces are correctly described [30,33,46,47] and static correlation effects can be incorporated without spuriously breaking the spin symmetry of the system [43]) is not complete. An unphysical repulsion between the atoms appears at a large but finite internuclear distance and the size consistency of the ACFDT functionals is not always guaranteed [43]. These failures are a signature of crude approximations to the XC kernel but, certainly, they must be sorted out in order to provide further support to the ACFDT for being the basis of a next generation of electronic structure methods.

To gain insight into some of these issues we will consider a model one-dimensional (1D) system: two spin- $\frac{1}{2}$ fermions bound by a harmonic potential $v_{\text{ext}}(x) = \frac{1}{2}kx^2$ and interacting through the repulsive potential $w(x_1, x_2) = -\frac{1}{2}(x_1 - x_2)^2$. This is the 1D equivalent of the so-called Moshinsky atom [52],

whose ground- and excited-state wave functions and eigenenergies can be analytically obtained by simply doing a change in variables that separates the center-of-mass and the relative-motion contributions to the two-particle wave functions. As we will see in this paper, the same holds for the ACFDT correlation energies under the RPA and using the exact exchange-only kernel (EXK) $f_{\text{X},\gamma} = \gamma\delta v_{\text{X}}/\delta n$, where v_{X} is the exact time-dependent exchange potential [53]. Thus, although the fermion-fermion interaction of the Moshinsky atom is not realistic at all, this system is an ideal scenario to explore fundamental aspects of ACFDT advanced energy functionals.

The outline of the paper is as follows. In Sec. II we will present the exact results for the 1D Moshinsky atom that will be used in the rest of the paper. Section III will be devoted to the performance of the RPA and EXK correlation energies when evaluated over the exact density profiles, whereas the self-consistent implementation of these functionals will be discussed in Sec. IV. In Sec. V we will analyze the results obtained from the *exact* static XC kernel within the ACFDT framework. The corresponding conclusions will close the paper.

II. SOME EXACT RESULTS

The Hamiltonian of our model system is

$$H = \sum_{i=1}^2 \left(-\frac{1}{2} \frac{\partial}{\partial x_i^2} + \frac{1}{2} k x_i^2 \right) - \frac{\gamma}{2} (x_1 - x_2)^2, \quad (5)$$

with x_i being the coordinate of the i th fermion (we use a system of “atomic” units where $\hbar = m = 1$, with m being the fermion mass) and where we have introduced a dimensionless interaction strength $0 \leq \gamma \leq 1$. As mentioned in the introduction, this is a simple solvable model that has been often used to explore the nature of correlations in interacting fermion systems. Therefore, some of the results that will be presented in this section are well known, but mainly restricted to the three-dimensional case (see, for instance, the recent works by March *et al.* [54–59] and references therein). Furthermore, to the best of our knowledge a detailed description of the exact correlation energy functional including its relation to the adiabatic connection theorem [21,22,60] has not presented so far for the Moshinsky atom. Thus, it is worthwhile to present in this section all the relevant exact results that will be used in our subsequent analysis.

By doing the unitary change in coordinates $X = (x_1 + x_2)/\sqrt{2}$, $\varkappa = (x_1 - x_2)/\sqrt{2}$, original Hamiltonian (5) is transformed into the trivial one corresponding to two uncoupled harmonic oscillators with frequencies $\omega_{\text{ext}} = \sqrt{k}$ and $\omega_{\text{int}} = \sqrt{k - 2\gamma}$. Thus, the exact spacial eigenfunctions and eigenenergies can be labeled with two quantum numbers $n = 0, 1, 2, \dots$ and $l = 0, 1, 2, \dots$ in such a way that

$$\Psi_{nl}(x_1, x_2) = \eta_n \left(\omega_{\text{ext}}, \frac{x_1 + x_2}{\sqrt{2}} \right) \eta_l \left(\omega_{\text{int}}, \frac{x_1 - x_2}{\sqrt{2}} \right),$$

$$E_{nl} = \left(n + \frac{1}{2}\right)\omega_{\text{ext}} + \left(l + \frac{1}{2}\right)\omega_{\text{int}}, \quad (6)$$

with $\eta_i(\omega, x)$ being the i th eigenorbital of a 1D harmonic oscillator with mass $m=1$ and frequency ω . Note that the quantum number l defines the parity of $\eta_l(\omega_{\text{int}}, x)$, and as a consequence, the symmetric or antisymmetric character of Ψ_{nl} upon the exchange of spacial coordinates. That is, the spin state(s) of the energy level nl must be a singlet (triplet) if l is even (odd). In particular, the ground state $n=l=0$ is a singlet whose energy and spacial wave function are

$$E_g = \frac{\omega_{\text{ext}} + \omega_{\text{int}}}{2} = \frac{\sqrt{k} + \sqrt{k-2\gamma}}{2}, \quad (7)$$

$$\Psi_g(x_1, x_2) = \mathcal{N} \exp\left(-\frac{\omega_{\text{ext}}x_1^2 + \omega_{\text{int}}x_2^2}{2}\right), \quad (8)$$

with $\mathcal{N} = (\omega_{\text{ext}}\omega_{\text{int}}/\pi^2)^{1/4}$ being a normalization constant. Note that $k_{\text{crit}}=2\gamma$ is a critical value since the external potential can bind the two particles only if $k > k_{\text{crit}}$.

The ground-state expectation values of the kinetic, external, and interaction energies are

$$\begin{aligned} \langle \hat{T} \rangle_g &= \frac{\omega_{\text{ext}} + \omega_{\text{int}}}{4} = \frac{\sqrt{k} + \sqrt{k-2\gamma}}{4}, \\ \langle \hat{V}_{\text{ext}} \rangle_g &= \frac{\omega_{\text{ext}}\omega_{\text{int}} + \omega_{\text{ext}}^2}{4\omega_{\text{int}}} = \frac{\sqrt{k}\sqrt{k-2\gamma} + k}{4\sqrt{k-2\gamma}}, \\ \langle \hat{W} \rangle_g &= \frac{\omega_{\text{int}}^2 - \omega_{\text{ext}}^2}{4\omega_{\text{int}}} = \frac{-\gamma}{2\sqrt{k-2\gamma}}, \end{aligned} \quad (9)$$

respectively, and the ground-state density is

$$n_g(x) = 2|\eta_0(\Omega_g, x)|^2 = 2\left(\frac{\Omega_g}{\pi}\right)^{1/2} \exp(-\Omega_g x^2) \quad (10)$$

where

$$\Omega_g = \frac{2}{\omega_{\text{ext}}^{-1} + \omega_{\text{int}}^{-1}} = \frac{2}{k^{-1/2} + (k-2\gamma)^{-1/2}}. \quad (11)$$

It is also straightforward to get the exact values of the KS kinetic, external, Hartree, exchange, and correlation energies:

$$\begin{aligned} T_S(k, \gamma) &= \frac{\sqrt{k}\sqrt{k-2\gamma}}{\sqrt{k} + \sqrt{k-2\gamma}} = \frac{\Omega_g}{2}, \\ V_{\text{ext}}(k, \gamma) &= \frac{1}{4}\left(\sqrt{k} + \frac{k}{\sqrt{k-2\gamma}}\right) = \frac{k}{2\Omega_g}, \\ W_H(k, \gamma) &= -\frac{\gamma}{2}\left(\frac{1}{\sqrt{k}} + \frac{1}{\sqrt{k-2\gamma}}\right) = -\frac{\gamma}{\Omega_g}, \\ E_X(k, \gamma) &= -\frac{1}{2}W_H(k, \gamma), \end{aligned}$$

$$E_C(k, \gamma) = W_C(k, \gamma) + T_C(k, \gamma), \quad (12)$$

where $T_C(k, \gamma)$ and $W_C(k, \gamma)$ are the kinetic and the potential (or the interaction energy) contributions to $E_C(k, \gamma)$, respectively,

$$\begin{aligned} W_C(k, \gamma) &= \frac{\gamma}{4}\left(\frac{1}{\sqrt{k}} - \frac{1}{\sqrt{k-2\gamma}}\right), \\ T_C(k, \gamma) &= \frac{1}{4}\frac{(\sqrt{k} - \sqrt{k-2\gamma})^2}{\sqrt{k} + \sqrt{k-2\gamma}}. \end{aligned} \quad (13)$$

Equation (10) tells us that the exact KS system consists of two noninteracting fermions under the action of a harmonic potential with frequency Ω_g ,

$$v_S(x) = \frac{1}{2}\Omega_g^2 x^2 + \frac{\sqrt{k-2\gamma} - \Omega_g}{2}, \quad (14)$$

where we have added a constant to align the energy of the doubly occupied KS state with the exact ionization energy of the system $\sqrt{k-2\gamma}/2$. Reciprocally, a generic Gaussian density $n_\Omega(x) = 2|\eta_0(\Omega, x)|^2$ is the ground-state one of a system of two interacting fermions bound by an external harmonic potential whose frequency $\varpi(\Omega, \gamma)$ is given implicitly by the equation

$$\Omega = 2\left(\frac{1}{\varpi(\Omega, \gamma)} + \frac{1}{\sqrt{\varpi(\Omega, \gamma)^2 - 2\gamma}}\right)^{-1}. \quad (15)$$

This is a very simple illustration of the Hohenberg-Kohn theorem [2] which, in turn, also serves to find a number of exact expressions for density functionals if restricted to Gaussian densities. For instance, using Eqs. (13) and (15) we can see that $W_C^{(\gamma)}[n_\Omega]$ (the potential contribution to the correlation energy functional when the interaction strength is γ) is given by

$$W_C^{(\gamma)}[n_\Omega] = \frac{\gamma}{2\varpi(\Omega, \gamma)} - \frac{\gamma}{2\Omega}. \quad (16)$$

To help the reader when following the analysis below, the ground-state energy E_g and the frequency Ω_g that defines the ground-state density are plotted in Fig. 1 for $\gamma=1$ (full interaction between the fermions). For comparison we also include the self-consistent Hartree-Fock (HF) results $E_g^{\text{HF}} = \sqrt{\omega_{\text{ext}}^2 - 1}$ and $\Omega_g^{\text{HF}} = E_g^{\text{HF}}$ [61], as well as the exact XC and correlation energies [62]. As we may see, the smaller the value of ω_{ext} the more important the correlation effects, and the deviations between the exact and the HF results are fairly important even for finite ω_{ext} . The limit $\omega_{\text{ext}} \rightarrow \sqrt{2}$ corresponds to the onset of stability of the Moshinsky atom, where the performance of the HF approximation is extremely poor. Note that in this limit, the correlation energy diverges, whereas the XC one tends to $\sqrt{2}/2$.

Since we have considered arbitrary interaction strengths γ , the construction of the exact adiabatic-connection curve for any Gaussian ground-state density $n_\Omega(x)$ is straightforward. Indeed, according to the adiabatic connection theorem [21,22,60], $E_C[n]$ can be written exactly as

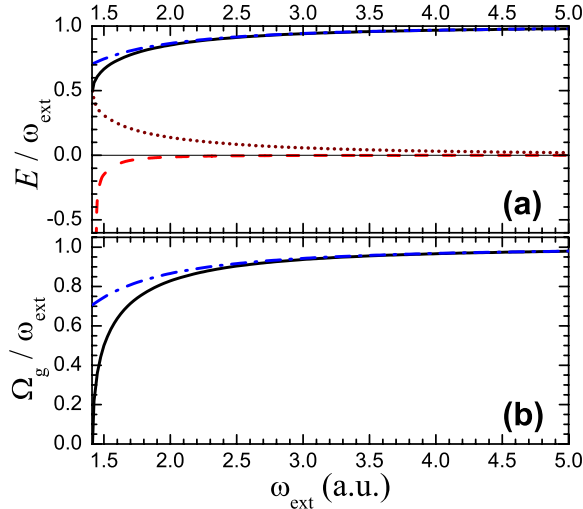


FIG. 1. (Color online) Upper panel: the exact (solid line) and HF (dash-dotted line) ground-state energies as a function of the frequency $\omega_{\text{ext}} = \sqrt{k}$ at full interaction strength ($\gamma=1$). The exact XC (dotted line) and the correlation (dashed line) energies are also included. Note that the XC energy is positive, whereas the correlation energy is negative and diverges in the limit $\omega_{\text{ext}} \rightarrow \sqrt{2}$. Lower panel: the exact (solid line) and HF (dash-dotted line) frequency Ω_g associated to the ground-state density.

$$E_C[n] = \int_0^1 d\gamma \frac{1}{\gamma} W_C^{(\gamma)}[n] \doteq \int_0^1 d\gamma U_C^{(\gamma)}[n], \quad (17)$$

and by simple substitution we arrive at the important relation

$$E_C[n_\Omega] = \int_0^1 d\gamma \left(\frac{1}{2\varpi(\Omega, \gamma)} - \frac{1}{2\Omega} \right) \\ = \frac{1}{2} \left(\frac{[\varpi(\Omega) - \Omega]^2}{2\varpi(\Omega) - \Omega} + \frac{1}{\varpi(\Omega)} - \frac{1}{\Omega} \right) \quad (18)$$

(note that if $\gamma=1$ then we skip any dependence on γ). Equation (18) illustrates the convenience of the Moshinsky model to study not only ACFDT functionals but also the adiabatic connection itself, which plays a central role in the foundations of DFT. In fact, such a study is not easy to carry out even for few-electron systems [63–66] since it is necessary to obtain the external potential that leads to the same ground-state density for the whole range of the interaction strengths.

The exact adiabatic connection curve [Eq. (18)] is represented in Fig. 2 for three different regimes: weak, intermediate, and high correlation. Whereas for weak correlation ($\Omega \gg 0$) $U_C^{(\gamma)}[n_\Omega]$ is almost a straight line (a signature of the accuracy of Görling-Levy second-order perturbation theory [12]), its curvature is already evident in the intermediate correlation regime. For small Ω , $U_C^{(\gamma)}[n_\Omega]$ quickly reaches an almost constant value which reflects that the interaction contribution W_C to the total correlation energy dominates over the kinetic one T_C . There is an apparent resemblance with the behavior of the adiabatic connection in the dissociation process of molecules [66]. However, for the highly correlated Moshinsky atom $T_C[n_g] \rightarrow \langle \hat{T} \rangle_g$, whereas, for instance, in the dissociated H_2 molecule $T_C[n_g] \rightarrow 0$. Actually, regarding the

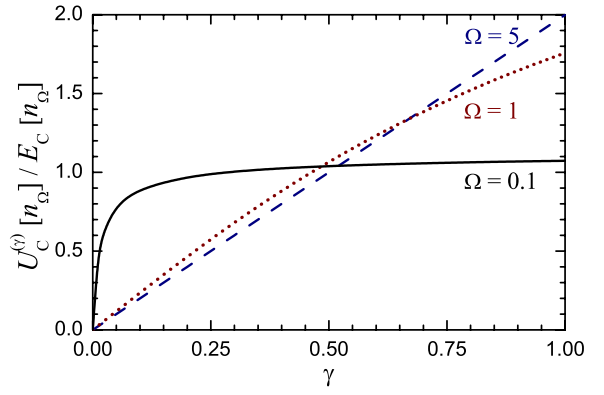


FIG. 2. (Color online) The exact adiabatic connection curve $U_C^{(\gamma)}[n_\Omega]/E_C[n_\Omega]$ for Gaussian densities $n_\Omega(x)$ with $\Omega=5, 1$, and 0.1 . These densities illustrate the weak (dashed line), intermediate (dotted line), and high (solid line) correlation regimes, respectively, and correspond to Moshinsky 1D atoms with $\omega_{\text{ext}}=5.102, 1.591$, and 1.415 . Note that the area under the curves is always equal to one.

nature of fermion correlations, the present model is much closer to the so-called Wigner molecules [67–69], where strong correlations lead to the appearance of electron localization effects.

III. TESTING THE RPA AND EXK

Let us consider a 1D Moshinsky atom whose exact ground-state density is $n_\Omega(x)$. As mentioned in the previous section, the corresponding KS system consists of two noninteracting fermions bound by a harmonic potential of frequency Ω . Then, the noninteracting KS response $\hat{\chi}_0(\omega)$ [Eq. (3)] can be written as

$$\chi_0(x_1, x_2; \omega) = \sum_{n=1}^{\infty} \zeta_n(x_1) g_n^{(0)}(\omega) \zeta_n(x_2) \quad (19)$$

(for the sake of simplicity, we omit the dependences on Ω). Here, $\zeta_n(x) = \eta_0(\Omega, x) \eta_n(\Omega, x)$ is a set of nonorthogonal orbitals and

$$g_n^{(0)}(\omega) = \frac{2}{\omega - n\Omega + i0^+} - \frac{2}{\omega + n\Omega + i0^+}. \quad (20)$$

$\hat{\chi}_0(\omega)$ can be seen as a frequency-dependent operator in the one-fermion Hilbert space:

$$\hat{\chi}_0(\omega) = \sum_{n=1}^{\infty} |\zeta_n\rangle g_n^{(0)}(\omega) \langle \zeta_n|, \quad (21)$$

and the interacting response $\hat{\chi}_\gamma(\omega)$ is, formally,

$$\hat{\chi}_\gamma(\omega) = \hat{\chi}_0(\omega) \sum_{M=0}^{\infty} \{ [\gamma \hat{w} + \hat{f}_{\text{XC}, \gamma}(\omega)] \hat{\chi}_0(\omega) \}^M. \quad (22)$$

The RPA neglects the XC kernel whereas the EXK for a two-fermion system is static and simply given by $-\gamma \hat{w}/2$. Then, under these approximations, the interacting response is

$$\hat{\chi}_\gamma^{\text{RPA/EXK}}(\omega) = \hat{\chi}_0(\omega) \sum_{M=0}^{\infty} [\xi \gamma \hat{w} \hat{\chi}_0(\omega)]^M. \quad (23)$$

where ξ is equal to 1 for the RPA and to $\frac{1}{2}$ for the EXK. This infinite summation can be done analytically just bearing in mind that for $n, m \geq 1$

$$\langle \zeta_n | \hat{w} | \zeta_m \rangle = \int dx_1 dx_2 \zeta_n(x_1) w(x_1, x_2) \zeta_m(x_2) = \frac{\delta_{n,1} \delta_{m,1}}{2\Omega}, \quad (24)$$

which implies that

$$\hat{\chi}_0(\omega) [\hat{w} \hat{\chi}_0(\omega)]^M = |\zeta_1\rangle \left(\frac{g_1^{(0)}(\omega)}{2\Omega} \right)^M g_1^{(0)}(\omega) \langle \zeta_1|. \quad (25)$$

Thus, by substituting Eq. (25) into Eq. (23) we have that

$$\hat{\chi}_\gamma^{\text{RPA/EXK}}(\omega) = \sum_{n=1}^{\infty} |\zeta_n\rangle g_n^{(\gamma)}(\omega) \langle \zeta_n|, \quad (26)$$

where $g_n^{(\gamma)}(\omega) = g_n^{(0)}(\omega)$ for $n \geq 2$ and

$$g_1^{(\gamma)}(\omega) = g_1^{(0)}(\omega) \sum_{M=0}^{\infty} \left(\frac{\xi \gamma g_1^{(0)}(\omega)}{2\Omega} \right)^M = \frac{\Omega}{\tilde{\Omega}} \left[\frac{2}{\omega - \tilde{\Omega} + i0^+} - \frac{2}{\omega + \tilde{\Omega} + i0^+} \right], \quad (27)$$

with $\tilde{\Omega} = \sqrt{\Omega^2 + 2\xi\gamma}$. That is, the poles of the RPA, EXK, and KS responses for Gaussian densities $n_\Omega(x)$ are the same (multiples of the frequency Ω) excepting the first one, which is Ω for the KS response and $\tilde{\Omega}$ for the approximate interacting ones. This result could have been also obtained from Eq. (24) and using Casida's formulation [70] of TDDFT.

The corresponding RPA and EXK excitation energies extracted from the full-interaction response ($\gamma=1$) can be compared with the exact ones, which we label using the quantum numbers n, l (l is even to preserve the spin symmetry):

$$\varepsilon_{nl}[n_\Omega] = E_{nl}[n_\Omega] - E_g[n_\Omega] = n\varpi(\Omega) + l\sqrt{\varpi(\Omega)^2 - 2} \quad (28)$$

(note how we emphasize the functional dependence on the ground-state density). Such a comparison is made in Fig. 3, where we plot the exact excitations energies [Eq. (28)], the EXK ones $\sqrt{\Omega^2+1}$, 2Ω , 3Ω , etc., and, for completeness, the first RPA excitation energy $\sqrt{\Omega^2+2}$. Focusing on the EXK, it is obvious that it is not able to describe the rich spectrum of the model system except for the excitation $\varepsilon_{10}[n_\Omega]$, which is very well reproduced in the weakly correlated regime $\Omega \gg 0$. In the highly correlated limit, however, such an agreement is worse. Of course, the simplicity of the approximated spectra is due to the absence of any frequency dependence in the XC kernel. This limitation is even evident for $\Omega \gg 0$: the multiplets of actual excitations are reduced to a single EXK or RPA excitation, a general behavior already described in detail by Maitra *et al.* [71].

Expression (26) can be also used to obtain the RPA and EXK correlation energies, one of the main objectives of the

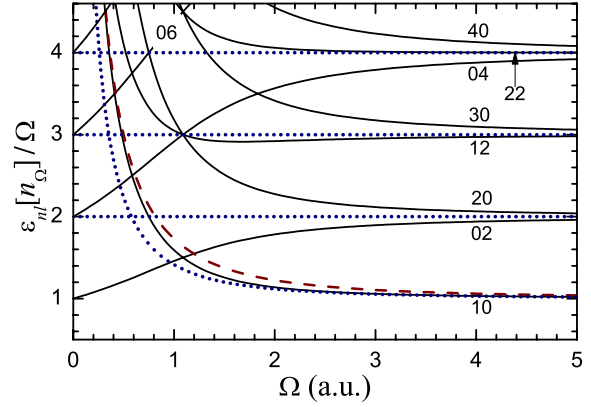


FIG. 3. (Color online) Exact excitation energies $\varepsilon_{nl}[n_\Omega]$ (solid lines labeled with the quantum numbers nl) for a 1D Moshinsky atom whose ground-state density is $n_\Omega(x)$. The EXK excitations (dotted lines) and the first RPA excitation (dashed line) evaluated from $n_\Omega(x)$ are also included. The EXK and RPA approximations are only able to account for the $n=1$, $l=0$ excitation which, in the highly correlated regime, is not the lowest one. All the other excitations correspond to nearly-degenerated multiplets in the limit $\Omega \gg 0$, and the description of such multiplets are completely out of the scope of EXK and RPA.

present work. Since $\Delta \hat{\chi}_\gamma(\omega) = \hat{\chi}_\gamma(\omega) - \hat{\chi}_0(\omega)$ is equal to $|\zeta_1\rangle [g_1^{(\gamma)}(\omega) - g_1^{(0)}(\omega)] \langle \zeta_1| \equiv |\zeta_1\rangle \Delta g_1^{(\gamma)}(\omega) \langle \zeta_1|$, we have that

$$U_C^{(\gamma)}[n_\Omega] = -\text{Im} \int_0^\infty \frac{d\omega}{2\pi} \int dx dx' w(x, x') \Delta \chi_\gamma(x, x'; \omega) \approx -\text{Im} \int_0^\infty \frac{d\omega}{2\pi} \langle \zeta_1 | \hat{w} | \zeta_1 \rangle \Delta g_1^{(\gamma)}(\omega). \quad (29)$$

Now, using Eqs. (24) and (27) and performing the integration over ω , we arrive at

$$U_C^{(\gamma)}[n_\Omega] \approx -\frac{1}{2} \left(\frac{1}{\Omega} - \frac{1}{\sqrt{\Omega^2 + 2\xi\gamma}} \right). \quad (30)$$

Finally, the integral over the interaction strength is immediate. The RPA or EXK $E_C[n_\Omega]$ functionals are

$$E_C^{\text{RPA/EXK}}[n_\Omega] = -\frac{1}{2\Omega} + \frac{\sqrt{\Omega^2 + 2\xi} - \Omega}{2\xi}, \quad (31)$$

and adding the exact exchange term $1/(2\Omega)$ we obtain the RPA/EXK XC functionals.

In Fig. 4 we represent the errors committed by the RPA and the EXK correlation functionals. As we may see, the RPA reproduces the exact limit of the correlation energy at $\Omega=0$ but there is an overall overestimation of $E_C[n_\Omega]$ (in absolute value) especially in the region around $\Omega \sim 0.6$. Then, the RPA absolute error decreases for higher Ω . However, the latter masks the known bad performance of the RPA correlation functional which, as can be observed in the inset of Fig. 4, is qualitatively worse as the frequency Ω increases. On the contrary, the EXK is not able to give the exact limit of the correlation energy in the stability onset since $\lim_{\Omega \rightarrow 0} E_{XC}^{\text{EXK}}[n_\Omega] = 1 \neq \sqrt{2}/2$, and this approximation is not accurate in the highly correlated regime. However, the EXK

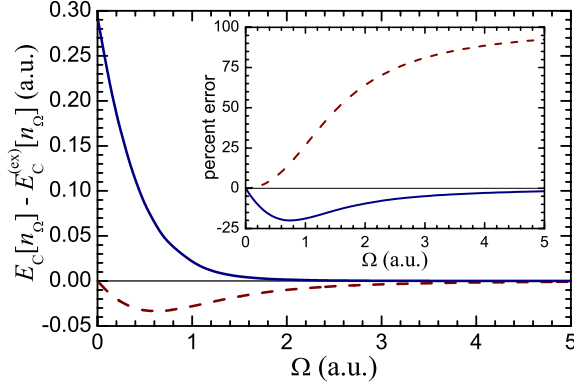


FIG. 4. (Color online) The absolute errors committed by the RPA (dashed lines) and the EXK (thick solid lines) when evaluating the correlation energy for a Gaussian density with frequency Ω . The inset shows the corresponding percent errors. Note the good performance of the EXK for intermediate and high values of Ω and the overall overestimation of the correlation energy (in absolute value) given by the RPA.

performs slightly better than the RPA for $\Omega \geq 1$ (where the EXK percent error in the correlation energy is around 20%) and shows its clear superiority when $\Omega \geq 2$, becoming a very good approximation to the correlation energy in the limit of weak interactions.

For our model system, the failure of the RPA when evaluating the correlation energy for weakly interacting systems can be easily traced back to the presence of self-interaction errors, practically eliminated by the EXK approximation. When the interaction is stronger, it is tempting to say that the failure of both ACFDT functionals is due to the absence of a frequency-dependent kernel since, as we have seen in Fig. 3, the actual excitation spectrum have nothing to do with the RPA/EXK ones. However, the good performance of the RPA in the highly correlated limit contradicts this statement. In fact, as we will see in Sec. V, it is possible to build an extremely accurate ACFDT correlation functional for this model system using a suitable static kernel.

IV. SELF-CONSISTENT RPA/EXK RESULTS

So far we have discussed the performance of the RPA and EXK ACFDT correlation functionals when evaluated over the exact ground-state density. However, such a density is not exactly known in practical applications and must be approximated as well. In the present model system, for instance, the HF density is fairly accurate if the fermion-fermion interaction is weak (see Fig. 1), but it is a poor approximation for intermediately ($1.5 \lesssim \omega_{\text{ext}} \lesssim 2$) and highly correlated ($\sqrt{2} < \omega_{\text{ext}} \lesssim 1.5$) Moshinsky atoms. Then, it is important to see to what extent the EXK and RPA are able to reproduce not only the energy, but also the ground-state density in those situations where mean-field approximations fail. To do so we need to solve the self-consistent Kohn-Sham equations, which requires the evaluation of the RPA/EXK correlation potential. Fortunately, as it is shown in detail in the Appendix, the RPA/EXK correlation potentials $v_C[n_\Omega](x)$ are quadratic (up to a constant) and the corresponding self-

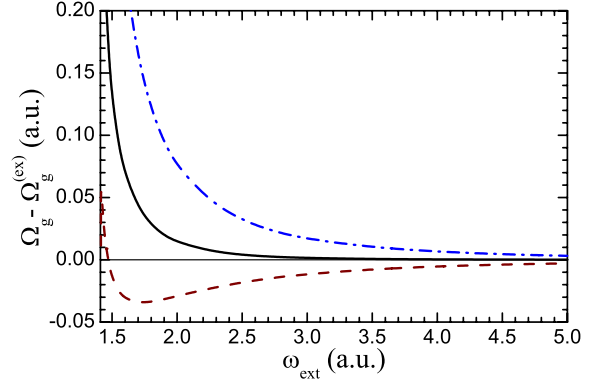


FIG. 5. (Color online) Absolute errors in the evaluation of the frequency Ω_g that defines the self-consistent ground-state densities using the HF (dash-dotted line), EXK (solid line), and RPA (dashed line) as a function of the frequency ω_{ext} of the external potential.

consistent densities are going to be Gaussians. Therefore, for a given external potential $v_{\text{ext}}(x) = \frac{1}{2}kx^2 = \frac{1}{2}\omega_{\text{ext}}^2 x^2$, the self-consistent resolution of the KS equation is equivalent to the minimization of the total-energy functional

$$E_{\text{tot}}[n] = T_S[n] + V_{\text{ext}}[n] + W_H[n] + E_X[n] + E_C[n] \quad (32)$$

over the set of two-electron Gaussian densities $n_\Omega(x)$. By using Eqs. (12) and (31), the RPA/EXK total-energy functional is

$$E_{\text{tot}}^{\text{RPA/EXK}}[n_\Omega] = \frac{\Omega}{2} + \frac{k-2}{2\Omega} + \frac{\sqrt{\Omega^2 + 2\xi} - \Omega}{2\xi}, \quad (33)$$

and the obtention of the frequency Ω_g that minimizes Eq. (33) is straightforward [72], whereas the corresponding ground-state energy is $E_g = E_{\text{tot}}[n_{\Omega_g}]$.

The quality of the self-consistent ground-state densities can be observed in Fig. 5, where we plot the differences between the approximate HF/RPA/EXK Ω_g and the exact one $\Omega_g^{(ex)}$. As anticipated in Fig. 1, the HF prescription always overestimates Ω_g and the ground-state densities are more concentrated around $x=0$ than they should be. The RPA overvalues the correlation effects and Ω_g is underestimated except in the region $\sqrt{2} < \omega_{\text{ext}} \lesssim 1.5$ where the trend is the opposite because, as commented before, the RPA correlation functional is exact in the limit $\omega_{\text{ext}} \rightarrow \sqrt{2}$. Finally, although the EXK performs poorly in this highly correlated regime, it always leads to a great improvement with respect to the HF. In fact, the EXK gives the most accurate densities if $\omega_{\text{ext}} \geq 1.8$, being practically exact in the weakly correlated limit.

The behavior of the self-consistent total energies is rather similar, as we can see in Fig. 6. The EXK is extremely accurate for weakly correlated Moshinsky atoms and only breaks down if $\omega_{\text{ext}} \lesssim 1.8$. The RPA overestimates correlation effects and is a better approximation than EXK only in the limit of strong interactions ($\sqrt{2} < \omega_{\text{ext}} \lesssim 1.5$). Finally, the impact of the self-consistent resolution of the KS equations is illustrated in the inset of Fig. 6, where we display the differences between the RPA/EXK total energies evaluated from HF densities and the self-consistent ones. Such differences

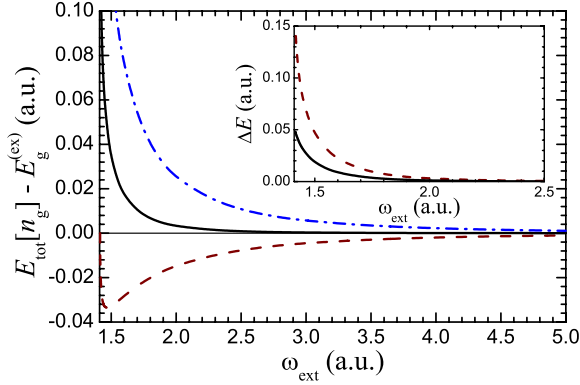


FIG. 6. (Color online) Absolute errors in the self-consistent evaluation of the total energy using the HF (dash-dotted line), the EXK (solid line), and the RPA (dashed line) as a function of the frequency ω_{ext} . The inset shows the difference $\Delta E = E_{\text{tot}}[n_g^{\text{HF}}] - E_{\text{tot}}[n_g]$ between the total energy evaluated over the HF density and the corresponding self-consistent one.

are negligible if $\omega_{\text{ext}} \geq 2$ which is, precisely, the region where the EXK total energies are very accurate. If $\omega_{\text{ext}} \leq 2$ the errors related to the lack of self-consistency are always less than the inherent ones if we consider the EXK functional. However, this post-HF implementation destroys the agreement between the RPA and the exact total energies in the highly correlated region. We can conclude that the performance of these ACFDT functionals is not affected very much if implemented in a non-self-consistent fashion in intermediately and weakly correlated systems. However, the good behavior exhibited by the RPA for highly correlated Moshinsky atoms is clearly compromised by the lack of self-consistency. Of course, this is not a surprise considering the very low quality of the mean-field densities in this regime.

V. EXACT ADIABATIC TDDFT RESULTS

The results of the preceding sections suggest that the quality of adiabatic ACFDT functionals (in the sense that they are built from frequency-independent kernels) is very sensible to changes in the structure of the excitation spectrum. However, the exact density response for the Moshinsky atom is

$$\chi(x, x'; \omega) = \sum_{nl}^{\text{unocc}} \rho_{nl}(x) \rho_{nl}(x') s_{nl}(\omega), \quad (34)$$

with $\rho_{nl}(x) = \langle \Psi_{nl} | \hat{n}(x) | \Psi_{00} \rangle / \sqrt{2}$ and $s_{nl}(\omega) = 2 \times [(\omega - E_{nl} + E_{00} + i0^+)^{-1} - (\omega + E_{nl} - E_{00} + i0^+)^{-1}]$ (for the sake of simplicity, we omit the dependences on the ground-state frequency Ω). Then, the potential contribution to the correlation energy [73],

$$W_C[n] = -\text{Im} \int_0^\infty \frac{d\omega}{2\pi} \int dxdx' w(x, x') \times [\chi(\mathbf{r}, \mathbf{r}'; \omega) - \chi_0(\mathbf{r}, \mathbf{r}'; \omega)], \quad (35)$$

can be rewritten sorting the excitations by multiplets, in such a way that

$$W_C[n_\Omega] = - \sum_{n=1}^\infty \int dxdx' w(x, x') \times \left[\zeta_n(x) \zeta_n(x') - \sum_{\substack{l=0 \\ l \text{ even}}}^n \rho_{n-l}(x) \rho_{n-l}(x') \right]. \quad (36)$$

Thus, the excitation energies do not appear explicitly in the evaluation of $U_C[n_\Omega]$ (although there is an implicit presence through, for instance, the f -sum rule). Therefore, the success of an ACFDT functional is more related to the proper account of the spectral weight of excitation multiplets than to the capability to describe the fine structure of such multiplets. In other words, as long as there is a fair correspondence between the approximated single excitations obtained from an adiabatic kernel and the actual multiplets of excitations, the corresponding ACFDT correlation functional can exhibit a good performance.

In our model system, it is easy to see (using some well-known properties of the Hermite polynomials [74]) that

$$\rho_{nl}(x) = b_{nl} \zeta_{n+l}(x), \quad (37)$$

where b_{nl} is a coefficient that actually depends on the frequency Ω of the Gaussian ground-state density. This implies that

$$\hat{\chi}(\omega) = \sum_{n=1}^\infty |\zeta_n\rangle \left[\sum_{\substack{l=0 \\ l \text{ even}}}^n b_{n-l}^2 s_{n-l}(\omega) \right] \langle \zeta_n | \doteq \sum_{n=1}^\infty |\zeta_n\rangle g_n^{(\text{ex})}(\omega) \langle \zeta_n | \quad (38)$$

and that

$$W_C[n_\Omega] = - \sum_{n=1}^\infty \langle \zeta_n | \hat{w} | \zeta_n \rangle \left[1 - \sum_{\substack{l=0 \\ l \text{ even}}}^n b_{n-l}^2 \right]. \quad (39)$$

Using Eq. (24) we have that [cf. Eq. (16)]

$$W_C[n_\Omega] = \frac{1}{2\Omega} (b_{10}^2 - 1) = \frac{1}{2\Omega} \left(\frac{\Omega}{\omega(\Omega)} - 1 \right) \quad (40)$$

and only the first excitation $n=1, l=0$ contributes to the correlation energy, an extreme case which is a mere consequence of the analytical features of the Moshinsky atom. In more realistic situations, many other (multiplets of) excitations will contribute to the correlation energy but, as stated before, what is important is the spectral weight of the multiplet and not its detailed structure. Also note that Eq. (40) explains the close correspondence between the accuracies of approximate correlation energies and $\varepsilon_{10}[n_\Omega]$ excitations that can be observed in Figs. 3 and 4.

A second consequence of Eq. (38) is that, necessarily,

$$\langle \zeta_n | \hat{w} + \hat{f}_{\text{XC}}(\omega) | \zeta_m \rangle = k_n(\omega) \delta_{n,m} \quad (41)$$

(i.e., exact Casida's equations are diagonal in the basis set $|\zeta_n\rangle$). Then, it is straightforward to see that

$$\langle \zeta_n | \hat{f}_{XC}(\omega) | \zeta_n \rangle = \frac{1}{g_n^{(0)}(\omega)} - \frac{1}{g_n^{(ex)}(\omega)} - \frac{\delta_{n,1}}{2\Omega} \quad (42)$$

and, in particular,

$$\langle \zeta_1 | \hat{f}_{XC}(\omega) | \zeta_1 \rangle = \frac{\varpi(\Omega)^2 - \Omega^2}{4\Omega} - \frac{1}{2\Omega}. \quad (43)$$

That is, the matrix element $\langle \zeta_1 | \hat{f}_{XC}(\omega) | \zeta_1 \rangle$ is frequency independent and tends to be zero (the RPA value) when $\Omega \rightarrow 0$ and to $-1/(4\Omega)$ (the EXK value) when $\Omega \gg 0$. We can immediately conclude that the exact adiabatic TDDFT leads to the exact correlation energies in the Moshinsky atom. Of course this will not be the case for other external potentials although it will be unlikely that a well-motivated adiabatic kernel would lead to a poor ACFDT correlation functional.

VI. CONCLUSIONS

In this paper we have studied the performance of the most popular implementations of the ACFDT to construct orbital-dependent correlation functionals. To do so we have chosen a very simple system, the 1D Moshinsky atom, in which many relevant analyses can be made analytically. We have seen that simple ACFDT functionals provide accurate correlation energies and self-consistent ground-state densities even when, due to the strength of the fermion-fermion interaction, mean-field approximations are completely inaccurate.

Fairly speaking, the Moshinsky atom is a very favorable scenario for ACFDT functionals. The multiplets of nearly-degenerated excitations do not contribute to the correlation energy and a frequency-dependent kernel is not actually needed to develop an accurate correlation functional. Moreover, the exact adiabatic kernel reproduces the correlation energies exactly. Nevertheless, we have arrived at some conclusions which could be useful in those (physical) systems where such multiplets do play a role. As an example, it is very easy that a model kernel $\hat{f}_{XC}(x, x'; \omega)$ could violate condition (41) thus wrongly mixing different multiplets of excitations and leading to spurious contributions to the correlation energy. Therefore, although it is possible to develop fairly accurate ACFDT functionals using either static [31,33] or dynamical [75] model XC kernels, these functionals could lead to unpredictable results in situations where there are very delicate energetics. The clearest example, which was mentioned in the introduction, is the artificial repulsion between atoms that appears at large interatomic separations. Then, it is likely that fully first-principles implementations of TDDFT aiming to reproduce all the features of excitation spectra and where dynamical XC kernels appear naturally [76] would be the only robust way to tackle these very stringent problems.

The analyses presented in this work were mainly focused on the ACFDT correlation functionals but can be also useful to study other fundamental issues. For instance, the performance of novel TDDFT approximations when predicting double-electron excitations or subtleties in the foundations of density-functional theory, such as chemical potential discontinuities [77], can be easily addressed for this model system.

Furthermore, as we will see in the Appendix, the *GW* self-energy operator is also analytical for the Moshinsky atom. Then, we are confident that the results presented in this paper will have further relevance in many current topics regarding the foundations of functional and many-body methods.

ACKNOWLEDGMENTS

The author is much obliged to the Spanish Ministry of Science and Technology for the financial support through the Ramon y Cajal Program and the research Grant No. FIS2007-65702-C02-02. Useful discussions with Rafael Almeida, José E. Alvarellos, Luis Chiva, Julio Fernández, Rex Godby, Héctor Mera, and Ángel Rubio are also acknowledged.

APPENDIX: RPA/EXK CORRELATION POTENTIALS

As it is well known [14,26–28], the RPA ($\xi=1$) and EXK ($\xi=\frac{1}{2}$) correlation potentials are given by the linearized Sham-Schlüter equation [78]

$$\int dx' \chi_0(x, x'; 0) v_C(x') = \Lambda_C(x), \quad (A1)$$

where $\chi_0(x, x'; 0)$ is the static KS linear response and

$$\begin{aligned} \Lambda_C(x) &= \int_{-\infty}^{+\infty} \frac{du}{\pi} \int dx'' G_0(x, x'; iu) \\ &\times \tilde{\Sigma}_C(x', x''; iu) G_0(x'', x; iu). \end{aligned} \quad (A2)$$

Here, G_0 is the KS one-electron Green's function and $\tilde{\Sigma}_C$ is an effective self-energy operator given by

$$\begin{aligned} \tilde{\Sigma}_C(x, x'; iu) &= - \int_{-\infty}^{+\infty} \frac{du'}{2\pi} e^{iu'0^+} G_0(x, x'; iu + i\nu) \\ &\times W_{sc}(x, x'; i\nu), \end{aligned} \quad (A3)$$

where $\hat{W}_{sc}(iu) = \hat{w} \hat{\chi}(iu) \hat{w}$. Note that we are using the imaginary-frequency representation instead of the real-frequency one.

For a Moshinsky atom whose ground-state density is $n_\Omega(x)$, the Kohn-Sham Green's function is

$$G_0(x, x'; iu) = \sum_{n=0}^{\infty} \frac{\eta_n(\Omega, x) \eta_n(\Omega, x')}{iu - \left(n - \frac{1}{2}\right)\Omega}, \quad (A4)$$

and, by using Eqs. (26) and (27), it is easy to see that

$$W_{sc}(x, x'; iu) = -\xi \left[\frac{2xx'}{u^2 + \tilde{\Omega}^2} + \frac{1}{2\Omega(u^2 + 4\Omega^2)} \right] \quad (A5)$$

[remember that $\tilde{\Omega} = (\Omega^2 + 2\xi)^{1/2}$]. As a consequence, the effective self-energy [Eq. (A3)] can be written as

$$\tilde{\Sigma}_C(x, x'; iu) = \xi \sum_{n=0}^{\infty} \eta_n(\Omega, x) \eta_n(\Omega, x') [A_n(iu)xx' + B_n(iu)], \quad (\text{A6})$$

and the functions $A_n(iu)$ and $B_n(iu)$ can be obtained by using Cauchy's theorem:

$$A_n(iu) = \frac{1}{\tilde{\Omega}} \frac{1}{iu - \left[\left(n - \frac{1}{2} \right) \Omega + \theta_n \tilde{\Omega} \right]},$$

$$B_n(iu) = \frac{1}{8\Omega^2} \frac{1}{iu - \left[\left(n - \frac{1}{2} \right) \Omega + 2\theta_n \Omega \right]}, \quad (\text{A7})$$

with $\theta_0 = -1$ and $\theta_{n \geq 1} = +1$. Note that the correlation contribution to Hedin's GW self-energy [79] is given by setting $\xi = 1$.

With these ingredients it is now possible to evaluate the function $\Lambda_C(x)$. To do so we only need to perform analytical integrals over the frequency u and to take into account that the position operator \hat{x} only connects harmonic oscillator eigenstates with consecutive quantum numbers and the relation $\eta_1(\Omega, x)^2 - \eta_0(\Omega, x)^2 = \eta_0(\Omega, x) \eta_2(\Omega, x) / \sqrt{2} = \zeta_2(x) / \sqrt{2}$. The result is

$$\Lambda_C(x) = \xi \frac{\tilde{\Omega} + 2\Omega}{\sqrt{2}\Omega^2(\Omega + \tilde{\Omega})^2} \zeta_2(x), \quad (\text{A8})$$

and from Eq. (A1) we have that

$$\sum_{n=1}^{\infty} \zeta_n(x) g_n^{(0)}(0) \int dx' \zeta_n(x') v_C(x') \propto \zeta_2(x). \quad (\text{A9})$$

Relation (A9) implies that $\int dx \zeta_n(x) v_C(x) = \int dx \eta_0(x) v_C(x) \eta_n(x)$ is zero except if $n=2$ (note that $n \geq 1$). Since the only local function that satisfies this condition is $v_C(x) = ax^2 + b$, it is then demonstrated that the RPA/EXK correlation potential for a Gaussian density is quadratic. The prefactor a can be obtained by simple identification of coefficients.

-
- [1] W. Kohn and L. Sham, *Phys. Rev.* **140**, A1133 (1965).
 [2] P. Hohenberg and W. Kohn, *Phys. Rev.* **136**, B864 (1964).
 [3] *A Primer in Density Functional Theory*, edited by C. Fiolhais, F. Nogueira, and M. A. L. Marques (Springer, Berlin, 2003), and references therein.
 [4] A. Görling, *J. Chem. Phys.* **123**, 062203 (2005).
 [5] S. Kümmel and L. Kronik, *Rev. Mod. Phys.* **80**, 3 (2008).
 [6] J. P. Perdew and Y. Wang, *Phys. Rev. B* **45**, 13244 (1992).
 [7] J. P. Perdew, K. Burke, and M. Ernzerhof, *Phys. Rev. Lett.* **77**, 3865 (1996).
 [8] J. P. Perdew, S. Kurth, A. Zupan, and P. Blaha, *Phys. Rev. Lett.* **82**, 2544 (1999).
 [9] J. Tao, J. P. Perdew, V. N. Staroverov, and G. E. Scuseria, *Phys. Rev. Lett.* **91**, 146401 (2003).
 [10] J. P. Perdew, A. Ruzsinszky, J. Tao, G. I. Csonka, and G. E. Scuseria, *Phys. Rev. A* **76**, 042506 (2007).
 [11] J. D. Talman and W. F. Shadwick, *Phys. Rev. A* **14**, 36 (1976).
 [12] A. Görling and M. Levy, *Phys. Rev. A* **50**, 196 (1994).
 [13] E. Engel, A. Facco Bonetti, S. Keller, I. Andrejkovics, and R. M. Dreizler, *Phys. Rev. A* **58**, 964 (1998).
 [14] E. Engel, in *A Primer in Density Functional Theory*, edited by C. Fiolhais, F. Nogueira, and M. A. L. Marques (Springer, Berlin, 2003).
 [15] E. Engel and H. Jiang, *Int. J. Quantum Chem.* **106**, 3242 (2006).
 [16] R. W. Godby and P. García-González, in *A Primer in Density Functional Theory*, edited by C. Fiolhais, F. Nogueira, and M. A. L. Marques (Springer, Berlin, 2003).
 [17] N. E. Dahlen and U. von Barth, *Phys. Rev. B* **69**, 195102 (2004).
 [18] U. von Barth, N. E. Dahlen, R. van Leeuwen, and G. Stefanucci, *Phys. Rev. B* **72**, 235109 (2005).
 [19] N. E. Dahlen, R. van Leeuwen, and U. von Barth, *Phys. Rev. A* **73**, 012511 (2006).
 [20] R. van Leeuwen, N. E. Dahlen, and A. Stan, *Phys. Rev. B* **74**, 195105 (2006).
 [21] H. -V. Nguyen and S. de Gironcoli, *Phys. Rev. B* **79**, 115105 (2009).
 [22] D. C. Langreth and J. P. Perdew, *Phys. Rev. B* **15**, 2884 (1977).
 [23] M. Lein, E. K. U. Gross, and J. P. Perdew, *Phys. Rev. B* **61**, 13431 (2000).
 [24] E. Runge and E. K. U. Gross, *Phys. Rev. Lett.* **52**, 997 (1984).
 [25] For a review see, for instance, *Time-Dependent Density Functional Theory*, edited by M. A. L. Marques, C. A. Ulrich, C. A. Nogueira, A. Rubio, K. Burke, and E. K. U. Gross (Springer, Berlin, 2006).
 [26] Y. M. Niquet, M. Fuchs, and X. Gonze, *Phys. Rev. A* **68**, 032507 (2003).
 [27] Y. M. Niquet, M. Fuchs, and X. Gonze, *J. Chem. Phys.* **118**, 9504 (2003).
 [28] Y. M. Niquet, M. Fuchs, and X. Gonze, *Int. J. Quantum Chem.* **101**, 635 (2005).
 [29] J. M. Pitarke and A. G. Eguiluz, *Phys. Rev. B* **57**, 6329 (1998).
 [30] J. F. Dobson and J. Wang, *Phys. Rev. Lett.* **82**, 2123 (1999).
 [31] J. F. Dobson and J. Wang, *Phys. Rev. B* **62**, 10038 (2000).
 [32] J. M. Pitarke and A. G. Eguiluz, *Phys. Rev. B* **63**, 045116 (2001).
 [33] J. Jung, P. García-González, J. F. Dobson, and R. W. Godby, *Phys. Rev. B* **70**, 205107 (2004).
 [34] P. García-González, J. J. Fernández, A. Marini, and A. Rubio, *J. Phys. Chem. A* **111**, 12458 (2007).
 [35] J. J. Fernández, J. Jung, W. Deakin, R. W. Godby, and P. García-González (unpublished).
 [36] H. Jiang and E. Engel, *J. Chem. Phys.* **127**, 184108 (2007).

- [37] M. Hellgren and U. von Barth, *Phys. Rev. B* **76**, 075107 (2007).
- [38] M. Hellgren and U. von Barth, *Phys. Rev. B* **78**, 115107 (2008).
- [39] F. Furche, *Phys. Rev. B* **64**, 195120 (2001).
- [40] M. Fuchs and X. Gonze, *Phys. Rev. B* **65**, 235109 (2002).
- [41] F. Aryasetiawan, T. Miyake, and K. Terakura, *Phys. Rev. Lett.* **88**, 166401 (2002).
- [42] M. Fuchs, K. Burke, Y. M. Niquet, and X. Gonze, *Phys. Rev. Lett.* **90**, 189701 (2003).
- [43] M. Fuchs, Y. M. Niquet, X. Gonze, and K. Burke, *J. Chem. Phys.* **122**, 094116 (2005).
- [44] F. Furche and T. Voorhis, *J. Chem. Phys.* **122**, 164106 (2005).
- [45] T. Miyake, F. Aryasetiawan, T. Kotani, M. van Schilfgaarde, M. Usuda, and K. Terakura, *Phys. Rev. B* **66**, 245103 (2002).
- [46] A. Marini, P. García-González, and A. Rubio, *Phys. Rev. Lett.* **96**, 136404 (2006).
- [47] J. Harl and G. Kresse, *Phys. Rev. B* **77**, 045136 (2008).
- [48] H.-V. Nguyen and S. de Gironcoli, e-print arXiv:0902.0889, *Phys. Rev. B* (to be published).
- [49] F. Furche, *J. Chem. Phys.* **129**, 114105 (2008).
- [50] A. G. Eguluz, M. Heinrichsmeier, A. Fleszar, and W. Hanke, *Phys. Rev. Lett.* **68**, 1359 (1992).
- [51] M. Grüning, A. Marini, and A. Rubio, *J. Chem. Phys.* **124**, 154108 (2006).
- [52] M. Moshinsky, *Am. J. Phys.* **36**, 52 (1968).
- [53] A. Görling, *Phys. Rev. A* **55**, 2630 (1997).
- [54] C. Amovilli and N. H. March, *Phys. Rev. A* **67**, 022509 (2003).
- [55] C. Amovilli and N. H. March, *Phys. Rev. A* **69**, 054302 (2004).
- [56] C. Amovilli and N. H. March, *Int. J. Quantum Chem.* **102**, 132 (2005).
- [57] N. H. March, J. Negro, and L. M. Nieto, *J. Phys. A* **39**, 3741 (2006).
- [58] A. Akbari, N. H. March, and A. Rubio, *Phys. Rev. A* **76**, 032510 (2007).
- [59] N. H. March, A. Cabo, F. Claro, and G. G. N. Angilella, *Phys. Rev. A* **77**, 042504 (2008).
- [60] O. Gunnarsson and B. I. Lundqvist, *Phys. Rev. B* **13**, 4274 (1976).
- [61] As it is well known, for two-fermion systems in a singlet spin state, the HF method is fully equivalent to the implementation of KS-DFT using the exact exchange [Eq. (1)] but neglecting the correlation. Thus, the exchange potential $v_X(\mathbf{r})$ and the Fock operator are the same and equal to $-\frac{1}{2}v_H(\mathbf{r})$ (the Hartree classical electrostatic potential). For the Moshinsky quadratic interaction, the Hartree potential generated by a Gaussian density is quadratic as well and the self-consistent solution of the HF equations leads to Gaussian ground-state densities. On the other hand, the relation $\Omega_g^{\text{HF}} = \sqrt{\omega_{\text{ext}}^2} - 1$ and the exact one [Eq. (11)] do not depend on the spacial dimension of the Moshinsky atom.
- [62] Remember that in the present context, the correlation energy is not the difference between the exact and the HF ground-state energies.
- [63] R. J. Magyar, W. Terilla, and K. Burke, *J. Chem. Phys.* **119**, 696 (2003).
- [64] F. Zhang and K. Burke, *Phys. Rev. A* **69**, 052510 (2004).
- [65] J. Katriel, S. Roy, and M. Springborg, *J. Chem. Phys.* **121**, 12179 (2004).
- [66] M. J. G. Peach, A. M. Teale, and D. J. Tozer, *J. Chem. Phys.* **126**, 244104 (2007).
- [67] D. C. Thompson and A. Alavi, *Phys. Rev. B* **66**, 235118 (2002).
- [68] J. Jung and J. E. Alvarillos, *J. Chem. Phys.* **118**, 10825 (2003).
- [69] D. C. Thompson and A. Alavi, *Phys. Rev. B* **69**, 201302(R) (2004).
- [70] M. E. Casida, in *Recent Advances in Density Functional Methods*, edited by D. E. Chong (World Scientific, Singapore, 1996).
- [71] N. T. Maitra, F. Zhang, R. J. Cave, and K. Burke, *J. Chem. Phys.* **120**, 5932 (2004).
- [72] Also note that Eq. (33) gives the HF total-energy functional just by taking the limit $\xi \rightarrow 0^+$.
- [73] The analysis in the present section will be restricted to $U_C[n]$ since the results can be easily extended to the whole correlation energy just by rescaling $U_C[n]$.
- [74] I. S. Gradshteyn and I. M. Ryzhik, *Table of Integrals, Series, and Products* (Academic Press, Orlando, 1980).
- [75] L. A. Constantin and J. M. Pitarke, *Phys. Rev. B* **75**, 245127 (2007).
- [76] M. E. Casida, *J. Phys. Chem.* **122**, 054111 (2005).
- [77] H. Mera and K. Stobro, *Phys. Rev. B* **79**, 125109 (2009).
- [78] L. J. Sham and M. Schlüter, *Phys. Rev. Lett.* **51**, 1888 (1983).
- [79] L. Hedin, *Phys. Rev.* **139**, A796 (1965).